

Description and Evaluation of a Hydrometeorological Forecast System for Mountainous Watersheds

KENNETH J. WESTRICK,* PASCAL STORCK, AND CLIFFORD F. MASS

Department of Atmospheric Science, University of Washington, Seattle, Washington

(Manuscript received 3 May 2001, in final form 10 September 2001)

ABSTRACT

This paper describes and evaluates an automated riverflow forecasting system for the prediction of peak flows during the cool season of 1998–99 over six watersheds in western Washington. The forecast system is based on the Pennsylvania State University–National Center for Atmospheric Research (Penn State–NCAR) fifth-generation Mesoscale Model (MM5) and the University of Washington Distributed-Hydrology-Soil-Vegetation Model (DHSVM). The control simulation used the forecasts produced by the University of Washington's real-time MM5 forecasts system as input to the hydrologic model. A second set of simulations applied a correction scheme that reduced the long-term precipitation bias identified in the MM5 precipitation field. A third set of simulations used only those observations that are available in real time for forcing the hydrologic model. The various MM5–DHSVM forecasts are also compared with those issued by the National Weather Service Northwest River Forecast Center. Results showed that the observations-based simulation produced the most accurate peak flow forecasts, although it was susceptible to inadequate input data and the overdependence on the few available observations. The control simulation performed remarkably well, although several poor synoptic (MM5) forecasts, in addition to a model wet bias, produced a significant overprediction of peak flows over one watershed. The bias correction scheme did not prove worthwhile for peak flow forecasting, but may be useful for longer-term modeling studies where the emphasis is on long-term discharge rather than peak flow forecasting. A real-time updating procedure that incorporated meteorologic observations in the creation of initial hydrologic states showed considerable promise for forecast peak streamflow error reduction.

1. Introduction

Real-time streamflow forecasting remains a formidable challenge in the mountainous western United States, where flooding and its effects represent the single most damaging weather-driven phenomenon in the region. The scarcity of real-time rain gauge data (Groisman and Legates 1994), poor radar coverage for precipitation estimation (Westrick et al. 1999), and large orographically induced precipitation gradients (Tangborn and Rasmussen 1976) greatly complicate the forecasting of streamflow. In addition, mesoscale effects in and near complex terrain provide additional challenges. For example, downwind of major gaps in the Cascade Mountain range, temperatures can be more than 10°C colder than in nearby nongap locations (Steenburgh et al. 1997), a gradient that is often crucial for forecasting rain-on-snow (ROS) flood events.

A limited number of studies have examined whether

hydrologic models driven by mesoscale atmospheric models can provide reasonable streamflow forecasts in regions of complex terrain given that the precipitation forecasts used as input are accurate (Westrick and Mass 2001; Miller and Kim 1996). The capability to produce accurate forecasts in real time has yet to be demonstrated. Mesoscale models can simulate the orographically influenced spatial distribution of rainfall accurately, although biases in the precipitation fields exist (Colle et al. 1999, 2000). Mesoscale models can also capture the complex three-dimensional structure in the temperature and wind fields provided that they possess horizontal resolution fine enough to resolve major orographic features (Steenburgh et al. 1997; Westrick and Mass 2001).

This study evaluates the performance of a high-resolution streamflow forecast system configured for real-time application in western Washington State during the cool season of 1998–99. Moderate La Niña conditions prevailed throughout this period and provided a range of medium-to-high-flow events ideal for assessing the performance of the system. Given the importance of flood forecasting throughout this region, this paper will concentrate on the prediction of peak streamflows for a number of significant runoff events.

The next section describes the atmospheric and hy-

* Current affiliation: 3TIER Environmental Forecasting Group Inc., Seattle, Washington.

Corresponding author address: K. J. Westrick, 2366 Eastlake Ave. East, Suite 415, Seattle, WA 98102.
E-mail: kwestrick@3tiergroup.com

drologic models, provides a brief description of the regional geography and climate, and describes the modeling and evaluation method. Section 3 provides results from the real-time system, with a sensitivity experiment detailed in section 4. This is followed by the summary and conclusions in section 5.

2. Geographic description and event overview

The six watersheds configured in this study are located on the western (windward) flanks of the Cascade Mountain range (Figs. 1a, b) and consequently receive copious amounts of precipitation, ranging between 2 and 3 m of precipitation annually (Daly et al. 1994). The sizes of these watersheds range from 106 to 1849 km² (Table 1), thus providing a range of sizes for assessing the accuracy of a streamflow forecast system. In addition, a large fraction of the total basin area of each watershed is located in or near the transient rain-snow zone, thereby making accurate prediction of precipitate type crucial during significant runoff events. There are a number of meteorological observation locations within the region (Fig. 1c), including seven Natural Resources Conservation Service Snowpack Telemetry (SNOTEL), seven Surface Airway Observations (SAO), and 19 hourly National Weather Service Cooperative Observer Program (CO-OP) sites. Data from all the sites were used for the calibration and validation of the Distributed-Hydrology-Soil-Vegetation Model (DHSVM) system prior to its application in real-time flood forecasting.

The hydrologic system was evaluated for the period 1 October 1998–30 March 1999, a period during which this region typically receives more than 80% of its annual precipitation. During this particular period, moderate La Niña (cold episode) conditions prevailed. In the Pacific Northwest La Niña periods are usually associated with colder temperatures and heavier precipitation (Mote et al. 1999); consistently, during the study period Washington State had the fourth wettest December–March on record, with unusually high winter snow accumulations in the Cascade Mountains. Mount Baker (Fig. 1b) set a world record for annual snowfall with over 1200 in. (Redmond 2000), and river discharges averaged above normal throughout much of the winter season. Despite the above-average precipitation throughout this evaluation period, all of the significant peak runoff events were at or below the 2-yr recurrence level (Sumioka et al. 1998). The observed hydrograph for the Snoqualmie River at Snoqualmie Falls reveals that there was six well-defined high runoff events during the cool season (Fig. 2), all within the 2-month period between mid-November 1998 and mid-January 1999. The performance of the coupled modeling system in forecasting these peak flows is the focus of this paper.

3. Model descriptions and forecast analysis method

a. Atmospheric model

The University of Washington (UW) real-time modeling system is based on the Pennsylvania State University–National Center for Atmospheric Research (Penn State–NCAR) fifth-generation Mesoscale Model (MM5), and has been used at the UW for real-time regional weather forecasting since 1995. The MM5 is a sigma-coordinate mesoscale atmospheric model (Grell et al. 1995) that has been used extensively for both research and forecasting throughout the world. Since autumn 1997 the system has used a three-domain configuration: a large 36-km outer domain covering the eastern Pacific and western North America; a 12-km nest over southern British Columbia, Washington, and Oregon; and a 4-km high-resolution nest over western Washington. Only the 4-km MM5 output is used for the MM5–DHSVM simulations. Thirty-two vertical layers are used, with increased resolution in the planetary boundary layer (PBL). Initial and boundary conditions, available at 6-h intervals, were interpolated from the National Centers for Environmental Prediction (NCEP) Eta Model 104 grids (80-km horizontal \times 25-hPa vertical resolution) to the MM5 grid. The suite of model physics used during the period of this assessment includes

- the explicit ice microphysics scheme of Dudhia (1989),
- the Kain–Fritsch cumulus parameterization scheme (Kain and Fritsch 1990) (36- and 12-km nests only), and
- the Medium-Range Forecast (MRF) (Hong and Pan 1996) planetary boundary layer scheme.

The model physics have remained relatively unchanged over the past several years, facilitating the gathering and assessment of long-term statistics. One major finding is that the MM5, using the explicit ice microphysics scheme, overpredicts precipitation upwind of major orographic barriers throughout the region for light to moderate amounts (Colle et al. 1999, 2000). This bias is especially relevant for this study, as all of the evaluated watersheds are located on the western (upwind) side of the Cascade Mountain barrier. A procedure to remove this bias prior to forcing the hydrologic model is discussed in the appendix.

b. Hydrologic model

The hydrologic model used in this project is the DHSVM, which is a physically based distributed hydrologic model designed for use in a variety of geographical and environmental settings (Wigmosta et al. 1994) that has been extensively tested in regions of complex terrain (Bowling et al. 2000; Storck et al. 1995). The version used in this study incorporates ex-

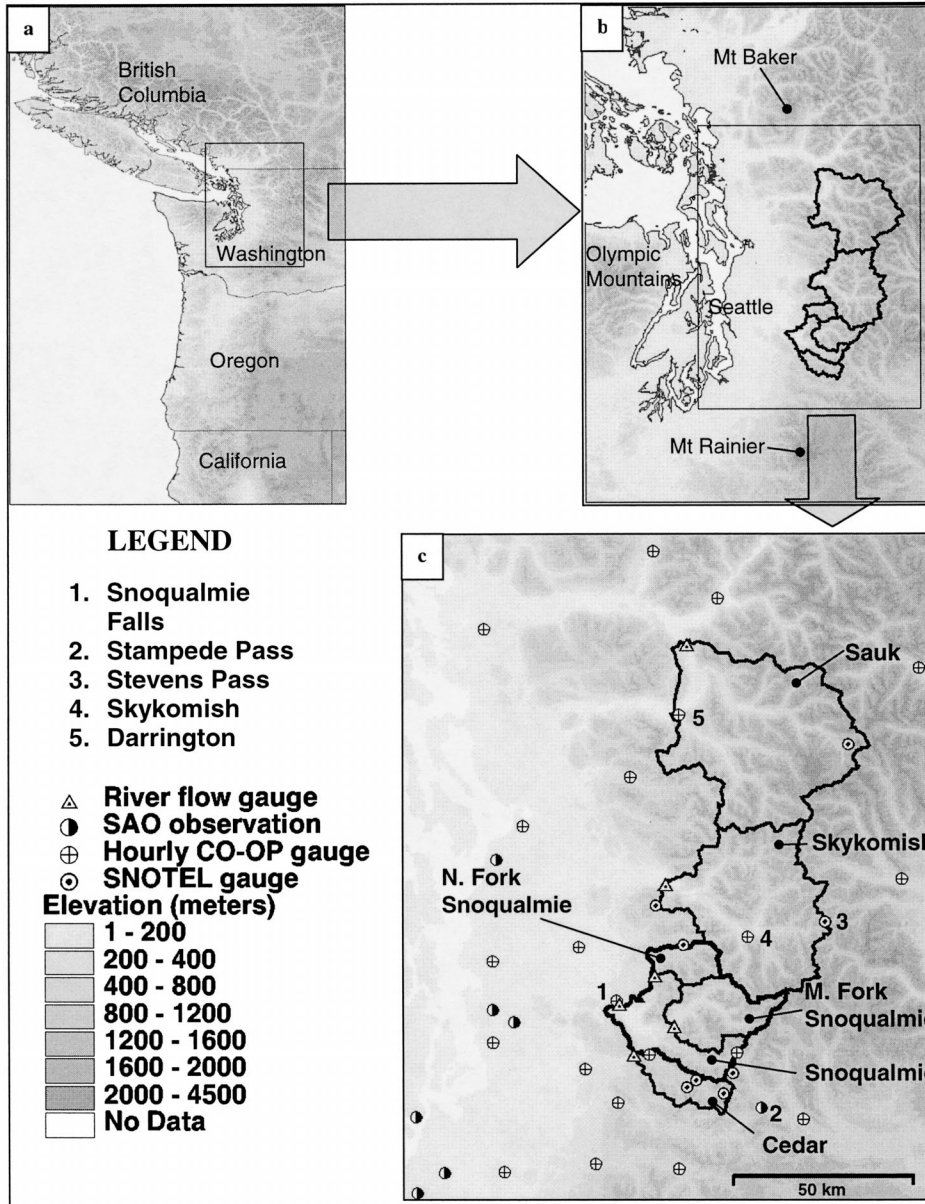


FIG. 1. Maps of (a) the Pacific Northwest, (b) western Washington, and (c) the western flanks of the Washington Cascade Mountains. The watersheds evaluated in this study are outlined in (b) and (c), with numbered locations in (c) identified in the legend.

plicit channel routing, allowing for the forecasting of streamflow at any point within the channel network. DHSVM includes an energy balance snowpack model that explicitly represents the effect of a forest canopy on snow accumulation and snowmelt (Storck and Lettenmaier 1999). The hydrologic model was configured at 150-m horizontal resolution and all hydrologic forecasts used a 1-h time step. A variable depth soil with three vertical layers was used, with the soil characteristics aggregated from the Conterminous U.S. Soil Dataset (Miller and White 1998). The land cover is derived from the 1991 Gap Analysis Program (GAP; Scott and

Jennings 1998) and allows for 19 separate land cover types.

DHSVM was calibrated with observed meteorological data using a 3-h time step for water years 1989–92. The 33 observation locations described in the previous section were used as meteorological input to DHSVM during the calibration. These observational data were thoroughly quality controlled (QC) with missing and/or bad data replaced using a variety of physically and statistically based methods (Westrick and Mass 2001). The Parameter-Elevation Regressions on Independent Slopes Model (PRISM) climatologic precipitation fields (Daly

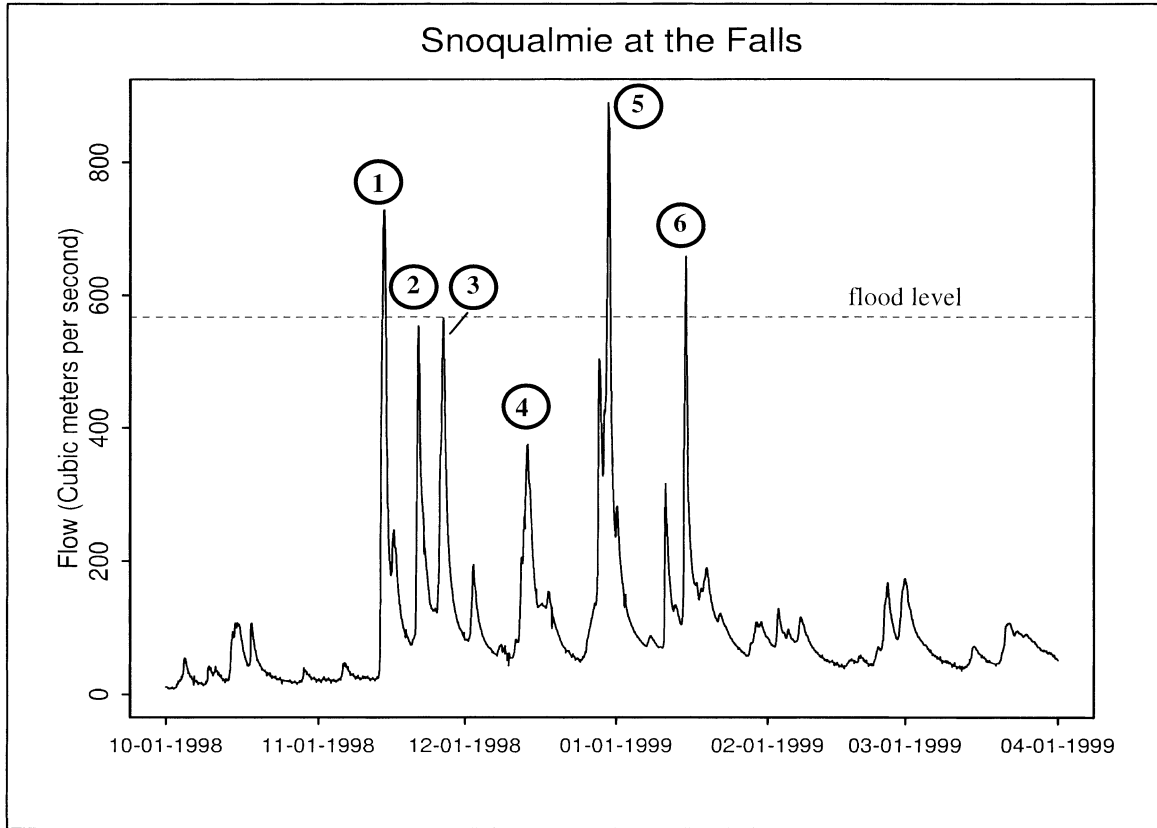


FIG. 2. Observed runoff on the Snoqualmie River at Snoqualmie Falls for the winter season 1998–99. The six peak flow events assessed in this study are event 1 (13–14 Nov 1998), event 2 (19–21 Nov 1998), event 3 (25–27 Nov 1998), event 4 (13–14 Dec 1998), event 5 (27–30 Dec 1998), and event 6 (13–15 Jan 1999).

et al. 1994) were used for spatially scaling the point precipitation data between observation points. Undercatchment of precipitation due to wind speed and precipitate type was corrected for using formulas from Yang et al. (1998).

The U.S. Geological Survey (USGS) gauge locations

on the Skykomish River at Gold Bar (not shown) and the Snoqualmie River at Carnation (Fig. 3a), Washington, were used for calibration. Calibration was limited to parameters controlling the distribution of soil moisture storage such as the total soil depth and saturated hydraulic conductivity, the distributions of which are

TABLE 1. Streamflow gauge locations, National Weather Service ID number, USGS ID number, drainage size, and peak flow for the six significant runoff events for water year 1999 [bold = 2–10-yr recurrence interval (Sumioka et al. 1998)].

| Name | NWS gauge ID No. | USGS gauge ID No. | Drainage size (km ²) | Significant events peak flow (m ³ s ⁻¹) | | | | | |
|--|------------------|-------------------|----------------------------------|--|----------------|----------------|----------------|----------------|----------------|
| | | | | 1 | 2 | 3 | 4 | 5 | 6 |
| | | | | 13–14 Nov 1998 | 19–21 Nov 1998 | 25–27 Nov 1998 | 13–14 Dec 1998 | 27–30 Dec 1998 | 13–15 Jan 1999 |
| Sauk River near Sauk | SAK | 12189500 | 1849 | 333 | 481 | 397 | 714 | 827 | 784 |
| Skykomish River near Gold Bar | GLB | 12134500 | 1385 | 902 | 661 | 520 | 557 | 1757 | 1206 |
| North Fork of the Snoqualmie River near Snoqualmie | SNQ | 12142000 | 166 | 179 | 147 | 127 | 99 | 209 | 196 |
| Snoqualmie River near Snoqualmie Falls | SQU | 12144500 | 971 | 728 | 553 | 565 | 183 | 889 | 658 |
| Middle Fork of the Snoqualmie River near Tanner | TAN | 12141300 | 399 | 479 | 364 | 299 | 375 | 507 | 422 |
| Cedar River near Cedar Falls | CRR | 12115000 | 106 | 41 | 52 | 54 | 19 | 121 | 59 |

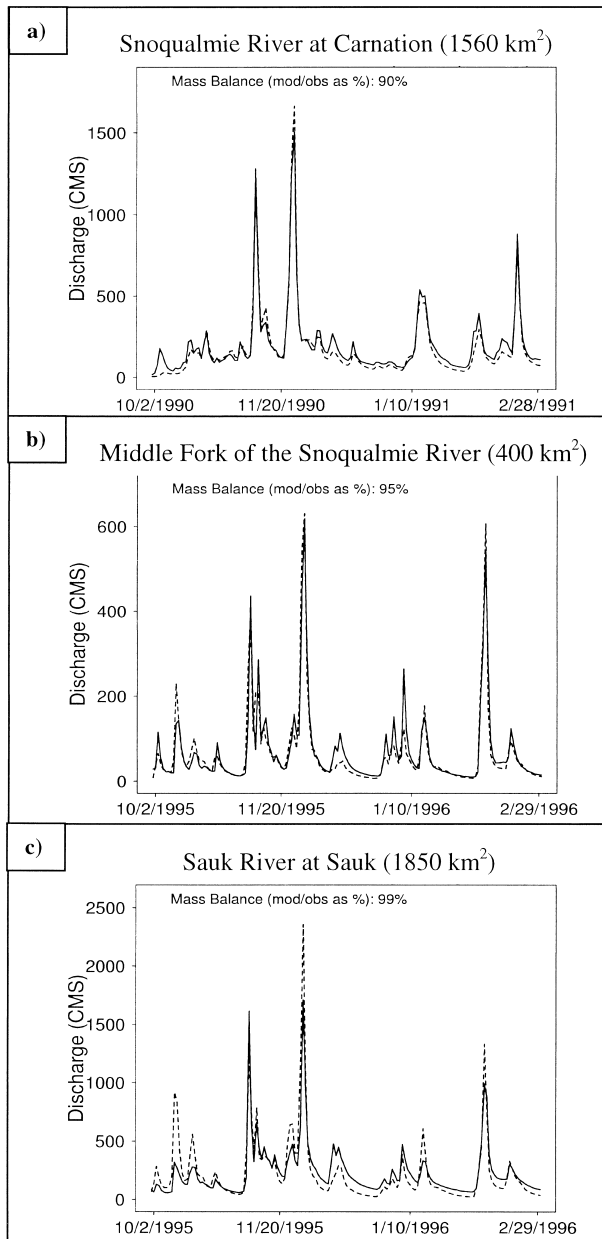


FIG. 3. Observed (solid) and model-predicted (dashed) hydrographs for the calibration period for the USGS gauge site at (a) Carnation, WA, and representative validation results for the cool season of 1995–96 at an uncalibrated location within (b) the same watershed (Middle Fork of the Snoqualmie River) and (c) in a nearby watershed (Sauk River at Sauk).

largely unknown at watershed scale. Previous studies (Storck et al. 1998), as well as sensitivity experiments conducted by the authors, have shown that these hydrological parameters had the greatest impact on peak runoff. Using the calibration parameters for Gold Bar and Carnation, the DHSVM model was then validated against observed runoff for water years 1992–96 at 17 USGS gauge locations on six river systems throughout western Washington. Analysis of the validation period

with the available daily mean flows at all USGS gauge sites revealed that the parameters developed for the two calibration sites transferred well to the validation watersheds. Representative results are shown for locations within (Fig. 3b) and outside (Fig. 3c) the calibration watershed for the winter of 1996 (during which two major flood events occurred, November 1995 and February 1996).

c. Forecast and analysis methods

This study evaluates the performance of the MM5–DHSVM coupled system for the period 1 October 1998–30 March 1999. Initial hydrologic states¹ for 1 October 1998 were created from an observation-driven DHSVM simulations conducted from 1 June to 30 September 1998. Prognostic model fields from the UW real-time MM5 forecast system were subsequently used to provide the meteorological fields for DHSVM. The required hydrologic fields, including soil moisture, snowpack, and interception, are carried forward in time with no updating by observations. All MM5-based hydrological forecasts use the 13–24-h forecast fields. The various configurations tested for this evaluation are as follows.

- *Direct MM5 input*—This forecast uses the MM5 forecast meteorological fields after they have been down-scaled (interpolated) to the 150-m resolution of the hydrologic model. Downscaling of the various 4-km horizontal-resolution MM5 forecast fields is accomplished through either bipolar interpolation (non-precipitation fields) or modified Cressman (precipitation fields) algorithms (Westrick and Mass 2001). This forecast will be referred to as the control simulation throughout this paper. The MM5 forecast of lowest sigma level (0.995σ) air temperature was adjusted using a model-derived lapse rate to compensate for the difference between the atmospheric model (MM5 at 4-km horizontal resolution) and hydrologic model (DHSVM at 150-m horizontal resolution) terrain heights.
- *Long-term MM5 precipitation bias removed*—In this sensitivity forecast a correction field that removes the long-term model precipitation bias is applied to all MM5 forecast precipitation fields. The bias correction method is described in the appendix.
- *DHSVM forced with observations only*—There is a time lag between when precipitation occurs over a watershed and when it arrives at a particular gauge site. This lag often allows for short-term hydrologic forecasts to be created based on observations, although the forecast period is limited to the time lag, which may be only a few hours. Because these forecasts use actual, rather than predicted meteorological

¹ The initial hydrologic states that DHSVM requires are soil moisture, snow quantity and quality, water intercepted by various vegetative layers, and quantity of water in the channel network.

conditions, this approach is likely to have greater predictive skill than a hydrologic forecast that is based on a meteorologic forecast. This configuration of the system uses observations from available SAO, SNOTEL, and hourly CO-OP precipitation sites to create the meteorological forcing for DHSVM (with no MM5). This configuration was performed with two objectives in mind: first, to assure that DHSVM can reproduce a similar degree of accuracy as was evident for the calibration-validation period (Figs. 3b, 3c), and second, to assess how the system performs when forced with observations available in real time. It should be noted that the number of observations used for this forecast was smaller than that used for calibration-validation, as fewer observations are available in real time.

To provide a performance benchmark for the UW system, the runoff forecasts produced by the National Weather Service Northwest River Forecast Center (NWS-NWRFC) are included for comparison. These forecasts were created using the National Weather Service River Forecast System (NWSRFS) with quantitative precipitation forecasts (QPFs) provided by the National Weather Service Forecast Offices, in this case, Seattle (NWSFO-SEA). The NWRFC forecasts used in this comparison were the forecasts valid 18–24 h from the time of issuance and are, therefore, comparable to the lead time of the MM5–DHSVM forecasts (13–24 h).

4. Results

For brevity, the various forecasts will be referred to as control (runoff forecasts that directly use MM5 forecast output), no bias (forecasts using the MM5 precipitation fields after processing with the bias reducing scheme described in the appendix), and observation based (using observations for meteorological forcing, as described in the previous section). The forecasts issued by the Northwest River Forecast Center will be referred to as RFC forecasts. The statistics shown below do not include forecast peak timing errors. This is due to the inherent difficulty in quantifying these types of errors, especially when updated forecasts are often made (in the case of the RFC forecasts) and in the case of complicated flood peaks (e.g., the case where two peaks are separated by 36 h but only differ by less than 1% in peak discharge). Unless otherwise noted, timing errors were at most 18 h and often much less. To provide more detail for the events of interest, the hydrograph figures will only encompass the time period from 10 November 1998 through 20 January 1999.

Figures 4 and 5 show the predicted and observed hydrographs for the various watersheds, and Table 2 provides detailed results for the peak flow events by watershed and event. For brevity, discussion of results will focus on major discrepancies or errors as well as noteworthy successes in the various forecasts.

The hydrograph for the Sauk River (Fig. 4a) reveals a significant overprediction in peak streamflow by both the control and no-bias forecasts for the first four events. For example, the observed peak streamflow for event 1 has a statistical recurrence of less than 2 yr, while the predicted peak has a recurrence of approximately 10 yr (Sumioka et al. 1998). Analysis of the hourly precipitation record from Darrington, the only rain gauge available within the Sauk River watershed (Fig. 1c, "5"), reveals that for the 4-day period from 12 to 15 November 1998, 74 mm (2.9 in.) of precipitation was observed, while the MM5 predicted 295 mm (11.3 in.) for the same time period. The peaks from the no-bias forecast are also significantly overpredicted. The substantial overprediction of this first event, and the subsequent oversaturation of the soils, adversely impacted the two subsequent events. The peak flows for events 2 and 3 are also substantially overpredicted because of both the soil oversaturation and a substantial overprediction of precipitation by MM5 (165 mm observed versus 427 mm predicted for the period 20–26 November). Also evident on the Sauk River is the substantial streamflow overprediction of event 4 by the control simulation due to excessive precipitation.

Of interest on the Skykomish River forecasts (Fig. 4b) is the inability of any of the forecasts to accurately capture event 5, with all forecasts capturing less than 60% of the peak flow. It is also worth noting both the timing and magnitude error for the observation-based forecast for event 5. Analysis of the Skykomish River rain gauge site (Fig. 1c, "4") reveals that 200 mm of precipitation fell from 24 to 27 December, while only 33 mm fell in the period 28–30 December, immediately before the observed flood peak on 30 December. This is in contrast to the SNOTEL site at Stevens Pass, which recorded 233 mm of precipitation during the 3-day period 28–30 December. It is likely that the precipitation values for the Skykomish River site were not representative of much of the watershed. Because of its central location within the Skykomish River watershed and the particular precipitation interpolation method used (inversed distance weighting), this site heavily affected the precipitation distribution.

Forecasts were better for the larger events on the North Fork of the Snoqualmie River (Fig. 4c), especially for the control simulation, although significant underforecasts for event 6 are noted. Substantial overprediction of event 5 for the North Fork of the Snoqualmie River is also evident in the RFC forecast. The results for the Middle Fork of the Snoqualmie River are quite similar to those of the North Fork (Fig. 5a), and the previously noted deficiency with the observation-based forecast for event 5 is still apparent. The Snoqualmie River at Snoqualmie Falls (Fig. 5b) is predicted quite well by all the forecast methods; this is especially apparent in the control simulation where all peak streamflow events forecast were within 22% of the observed.

The most accurate forecasts are produced for the Ce-

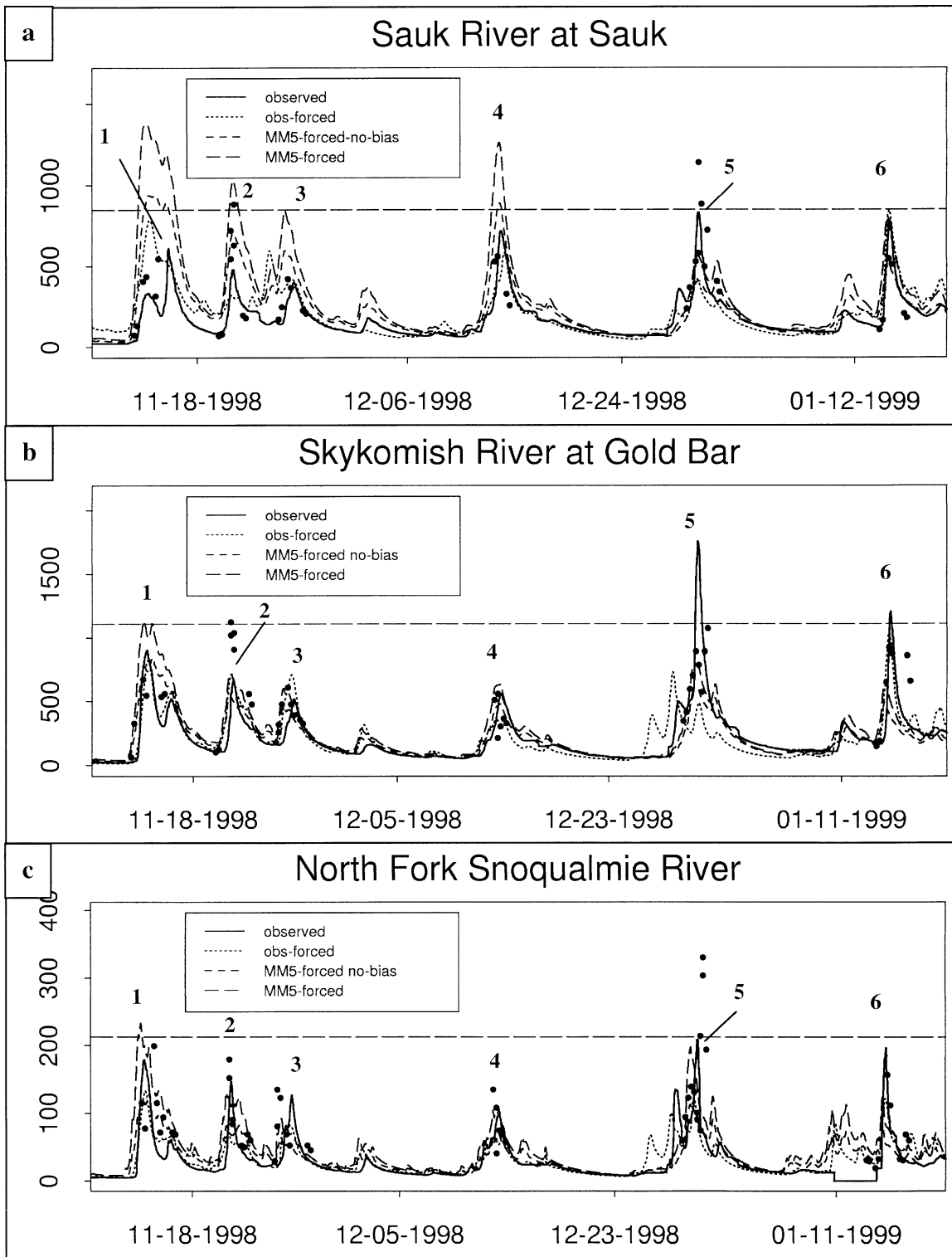


FIG. 4. Hydrographs of the observed and model-predicted hourly flows ($m^3 s^{-1}$) for the period 10 Nov 1998–20 Jan 1999 for USGS gauges at (a) the Sauk River at Sauk, (b) the Skykomish River at Gold Bar, and (c) the North Fork of the Snoqualmie River near Snoqualmie. The bold numbers refer to the six events described in the text. For comparison, the 18- and 24-h runoff forecasts issued by the NWRFC are also plotted (solid circles).

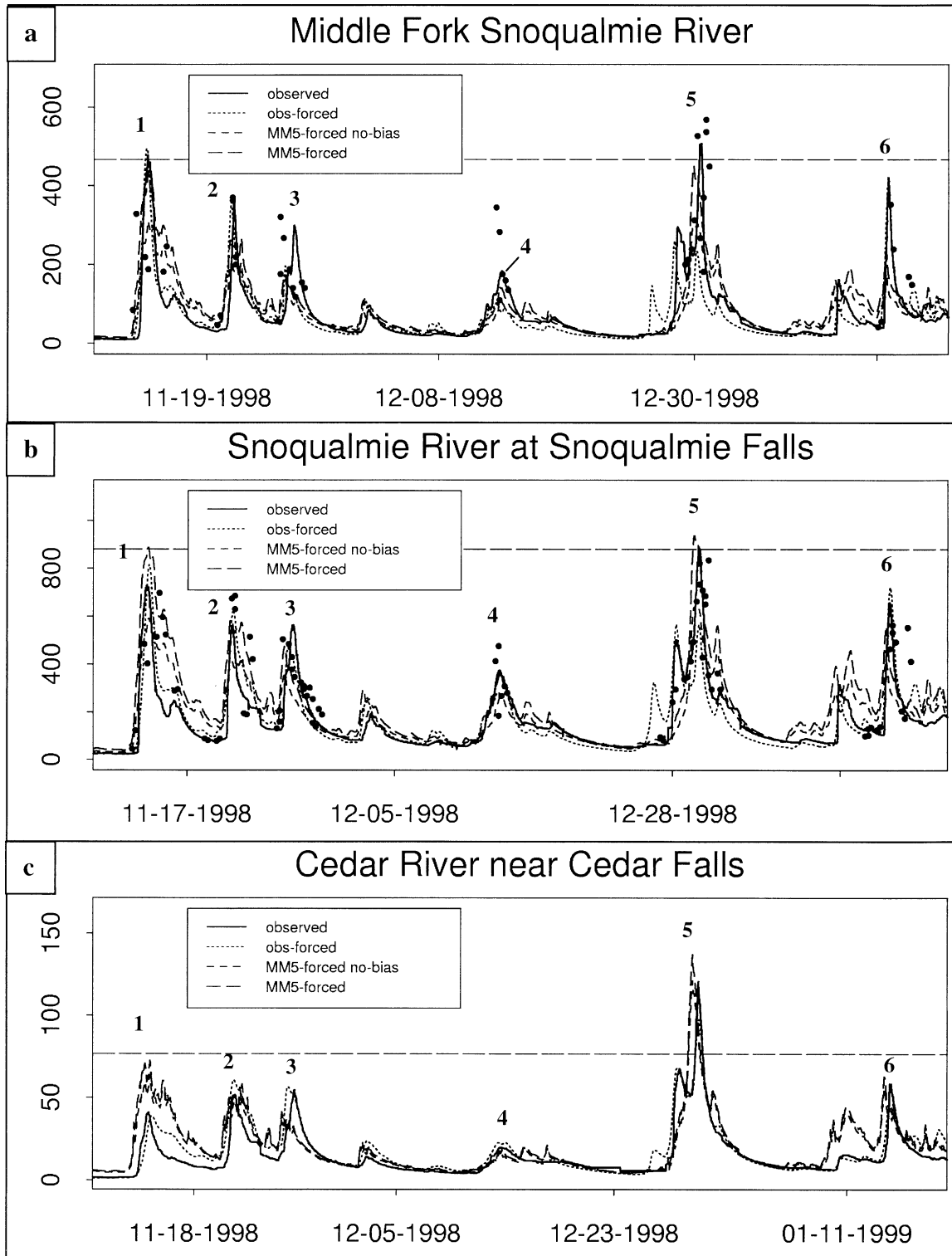


FIG. 5. As in Fig. 4 but for the following gauge sites: (a) the Middle Fork of the Snoqualmie River near Tanner, (b) the Snoqualmie River at Snoqualmie Falls, and (c) the Cedar River above Cedar Falls. NWRFC forecasts are not available for the Cedar River near Cedar Falls (c).

TABLE 2. Detailed breakdown of observed and predicted peak flows by event and watershed. Also shown are the peak relative error and the average absolute error by watershed.

| | Event 1 | | Event 2 | | Event 3 | | Event 4 | | Event 5 | | Event 6 | | Avg absolute error (%) | |
|--|--------------------|-----------|-----------|-----------|-----------|-----------|-----------|-----------|-----------|-----------|-----------|-----------|------------------------|------|
| | Peak flow | Error (%) | Peak flow | Error (%) | Peak flow | Error (%) | Peak flow | Error (%) | Peak flow | Error (%) | Peak flow | Error (%) | | |
| Sauk River near Sauk | Observed | 609 | 480 | 26.7 | 714 | 397 | 827 | 784 | 827 | 827 | 784 | 7.7 | 32.6 | |
| | Obs forced | 784 | 28.7 | 320 | -33.3 | 581 | 503 | 429 | 429 | 429 | 429 | 844 | 7.7 | |
| | MM5 forced | 1381 | 126.8 | 1030 | 114.6 | 1263 | 844 | 559 | 559 | 559 | 803 | 803 | 2.4 | 93.1 |
| | MM5 forced no bias | 939 | 54.2 | 703 | 46.5 | 888 | 596 | 407 | 407 | 407 | 534 | 534 | -31.9 | 51.6 |
| Skykomish River near Gold Bar | RFC forecast | 544 | -10.7 | 881 | 83.5 | 421 | 6.0 | 561 | 561 | 1140 | 544 | 544 | -30.6 | 38.0 |
| | Observed | 902 | 661 | 520 | 1757 | 1757 | 1206 | 1206 | 1206 | 1206 | 1206 | 1206 | -13.8 | 32.1 |
| | Obs forced | 823 | -8.8 | 715 | 8.2 | 709 | 36.3 | 361 | 361 | 730 | 1040 | 1040 | -44.4 | 32.7 |
| | MM5 forced | 1136 | 25.9 | 713 | 7.9 | 604 | 16.2 | 635 | 635 | 792 | 670 | 670 | -58.9 | 34.7 |
| North Fork of the Snoqualmie River near Snoqualmie | MM5 forced no bias | 848 | -6.0 | 537 | -18.8 | 482 | -10.2 | 482 | 482 | 590 | 496 | 496 | -39.0 | 35.2 |
| | RFC forecast | 675 | -25.2 | 1126 | 70.3 | 610 | 17.3 | 561 | 0.7 | 1072 | 923 | 923 | -23.5 | 35.2 |
| | Observed | 179 | 147 | 127 | 99 | 99 | 209 | 196 | 196 | 209 | 196 | 196 | -38.3 | 45.3 |
| | Obs forced | 133 | -25.7 | 71 | -51.7 | 82 | -35.4 | 65 | -34.3 | 123 | 121 | 121 | -36.7 | 23.8 |
| Middle Fork of the Snoqualmie River near Tanner | MM5 forced | 233 | 30.2 | 131 | -10.9 | 93 | -26.8 | 108 | 9.1 | 198 | 124 | 124 | -44.5 | 50.7 |
| | MM5 forced no bias | 127 | -29.1 | 82 | -44.2 | 65 | -48.8 | 70 | -29.3 | 116 | 83 | 83 | -20.4 | 30.9 |
| | RFC forecast | 199 | 11.2 | 180 | 22.4 | 135 | 6.3 | 135 | 36.4 | 330 | 156 | 156 | -1.4 | 27.2 |
| | Observed | 478 | 364 | 299 | 183 | 183 | 507 | 421 | 507 | 260 | 415 | 415 | -44.2 | 31.1 |
| Snoqualmie River near Snoqualmie Falls | Obs forced | 494 | 3.3 | 349 | -4.1 | 195 | -34.8 | 103 | -43.7 | 448 | 235 | 235 | -57.2 | 54.3 |
| | MM5 forced | 436 | -8.8 | 264 | -27.5 | 175 | -41.5 | 143 | -21.9 | 448 | 180 | 180 | 12.0 | 31.4 |
| | MM5 forced no bias | 309 | -35.4 | 197 | -45.9 | 138 | -53.8 | 107 | -41.5 | 315 | 353 | 353 | 56.3 | 22.6 |
| | RFC forecast | 328 | -31.4 | 370 | 1.6 | 321 | 7.4 | 345 | 88.5 | 568 | 658 | 658 | 9.6 | 13.4 |
| Cedar River near Cedar Falls | Observed | 727 | 553 | 564 | 375 | 375 | 889 | 564 | 889 | 567 | 721 | 721 | -14.7 | 34.3 |
| | Obs forced | 814 | 12.0 | 628 | 13.6 | 469 | -16.8 | 282 | -24.8 | 567 | 561 | 561 | -6.0 | 20.1 |
| | MM5 forced | 886 | 21.9 | 585 | 5.8 | 473 | -16.1 | 363 | -3.2 | 939 | 53 | 53 | -19.0 | 17.5 |
| | MM5 forced no bias | 600 | -17.5 | 427 | -22.8 | 359 | -36.3 | 263 | -29.9 | 637 | 417 | 417 | 6.8 | 26.7 |
| Cedar River near Cedar Falls | RFC forecast | 687 | -5.5 | 760 | 37.4 | 504 | -10.6 | 475 | 26.7 | 836 | 564 | 564 | -3.4 | 22.1 |
| | Observed | 41 | 51 | 54 | 19 | 19 | 121 | 59 | 121 | 98 | 46 | 46 | 0.0 | 17.5 |
| | Obs forced | 38 | -7.3 | 60 | 17.6 | 22 | 15.8 | 22 | 15.8 | 137 | 63 | 63 | 13.2 | 26.7 |
| | MM5 forced | 72 | 75.6 | 58 | 13.7 | 41 | -24.1 | 19 | 0.0 | 137 | 63 | 63 | 0.0 | 22.1 |
| Cedar River near Cedar Falls | MM5 forced no bias | 69 | 68.3 | 52 | 2.0 | 37 | -31.5 | 18 | -5.3 | 121 | 57 | 57 | -3.4 | 22.1 |

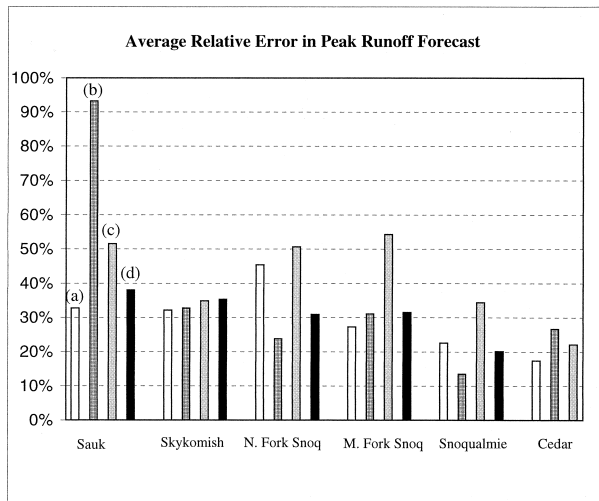


FIG. 6. The average absolute error in peak runoff forecast for six moderate runoff events during water year 1999. The errors are grouped by watershed. The forecasts are (a) observations based, (b) control, (c) no bias, and (d) the 18–24-h Northwest River Forecast Center model predictions, which are not available for the Cedar watershed.

dar River at Cedar Falls, where only event 1 has sizable errors. The results are especially encouraging when considering that the hydrologic system was calibrated for two watersheds that were an order of magnitude larger than the Cedar River system. Unfortunately, comparison RFC forecasts are not available for this watershed.

An assessment of the average peak error for the six events (Fig. 6) reveals that the observation-based configuration produced the most accurate forecasts, with an average error of 31%. This is not unexpected as it is the only forecast based on observed meteorological data. The fact that it is not significantly better than either the RFC or control forecasts suggests that uncertainties due to instrument error, areal representativeness of point observations, and the choice of interpolation method can be nearly as large as the uncertainty in the meteorological forecast, at least for a 13–24-h forecast.

It can also be seen that the observation-based forecast performs best on those river networks where the density of observations is highest (Fig. 1c), such as the Cedar and Snoqualmie Rivers, although it also performed remarkably well on the Sauk River watershed. Of the remaining forecasts, the control forecast had an average error for the six significant peaks of 38%, which was slightly worse than the RFC average forecast error of 32%. If the poor forecast on the Sauk River basin is excluded, the control forecast becomes the most accurate, with a forecast error of only 25%. The no-bias forecast had an average error of 45%, and nearly always erred on the low side. The poor performance of the no-bias forecast is due to the dependence of the precipitation bias on the synoptic-scale forcing (Colle et al. 1999, 2000). The precipitation bias is much more pronounced during weakly forced events and becomes

much less apparent during strongly forced events. Therefore, application of a single precipitation bias correction field reduces precipitation by a fixed fraction during all events and results in a degraded peak runoff forecast. Long-term mass balance is much better with the no-bias configuration though, as this configuration produced total 6-month runoff volumes that were much more accurate than the control and nearly as accurate as the observation-based forecast.

The significant overpredictions in streamflow on the Sauk River watershed were overwhelmingly due to poor MM5 meteorological forecasts. Since subsequent hydrological forecasts rely on previous forecasts for hydrological initial states, significant error can accumulate; thus a single poor MM5 forecast can adversely affect subsequent hydrological forecasts. To assess the benefits of more accurate hydrologic initial states in the forecast a test was conducted. In this test the hydrological forecasts are based on MM5-predicted meteorological conditions, but the initial hydrologic conditions for each forecast period are obtained from the observation-based hydrologic forecast. Although such a hybrid observation–MM5 forecast system can be implemented in real time, the value of such a system is highly dependent on the quality, representativeness, and real-time availability of the meteorological observations.

A significant improvement in streamflow forecasts is apparent when MM5-forced hydrologic states are regularly updated with an observation-based hydrologic forecast (Fig. 7). The dashed line indicates the original control forecast, and the open circles are the hourly forecasts from the updated initial state forecast. The error reduction is significant. For example, the peak error in the forecast for event 1 drops from greater than 120% to under 60% when the hydrologic model is initialized with observations-based initial states. There is also an indication of a second peak occurring early on 16 November, information that was not evident in the control forecast because of the severity of the peak flow error. Events 2 and 3 also show considerable improvement, and the relative error in the peak forecast error drops from 115% to 68% for event 2 and from 113% to 81% for event 3. Although overprediction of peak flow is still evident, this experiment does show that considerable reduction in peak error can result from using an observations-based initial hydrologic state.

5. Summary and conclusions

A coupled, fully automated atmospheric–hydrologic streamflow forecasting system using the Penn State–NCAR MM5 and the University of Washington distributed hydrologic model DHSVM is described. Three configurations of the system are evaluated for their ability to correctly forecast the peak discharge for six high-flow events during the cool season of 1998–99. The control configuration uses meteorological forecast fields from the 4-km-resolution nest of the MM5 as input to

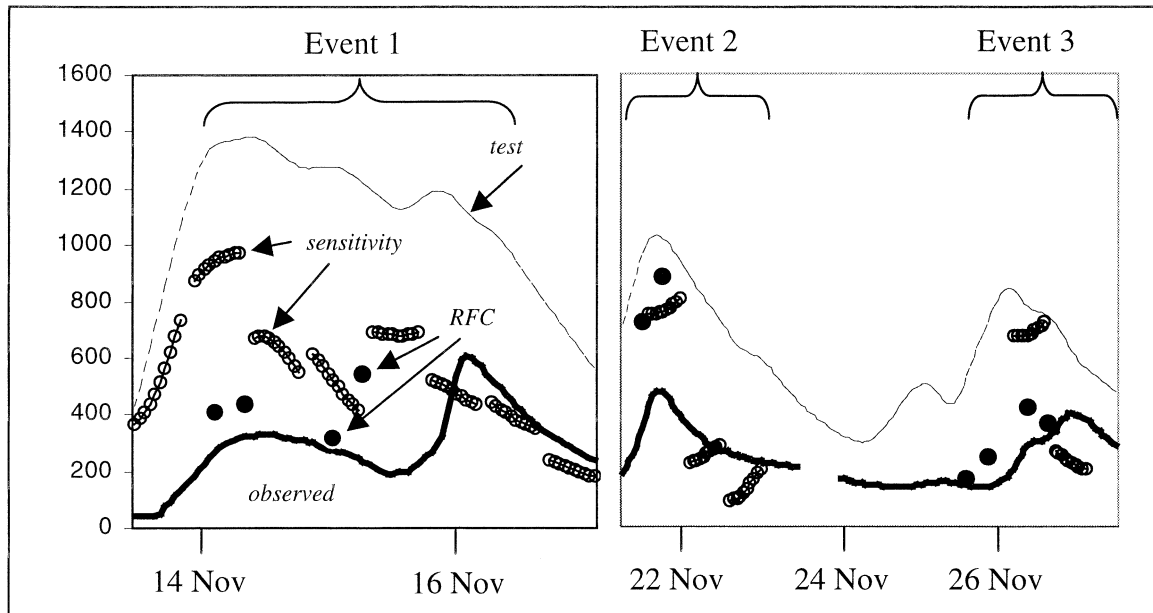


FIG. 7. Hydrographs of observed streamflow (heavy solid line), the control forecast (light dashed line), RFC forecast (solid black circles), and the test simulation that incorporated hydrologic initial states from the observations-based simulation (series of open circles denoted "sensitivity") for the Sauk River near the Sauk gauge site.

the distributed hydrological model. The second configuration uses the same system but applies a spatial-correction algorithm to remove the long-term precipitation bias when using this particular mesoscale model and microphysics scheme. The third configuration uses real-time meteorological observations rather than mesoscale model predictions to force the hydrological model. Riverflow forecasts issued by the National Weather Service Northwest River Forecast Center are also provided as a benchmark of performance for the system.

The hydrologic model was initially calibrated and then validated using observed meteorological data for a recent 8-yr period. The parameters developed for the two calibration watersheds transferred well to both larger and smaller watersheds within and outside of the original calibration watershed, with no further refinements to the original calibration parameters required.

Forecast results for the six high-flow events showed that the observations-based forecast performed best over all the basins, with an average error in peak flow of 31%.² The control, no-bias, and RFC forecasts had average errors of 38%, 45%, and 32%, respectively. On the Sauk River watershed the control forecast significantly overpredicted the peak flow for four of the six evaluated runoff events. The error was due to a series of poor synoptic weather forecasts by the mesoscale model, which overpredicted the observed precipitation by 200%–500% over this particular watershed. In ad-

dition to the synoptic error, the overprediction in precipitation was likely exacerbated by overproduction of precipitation by the mesoscale model (Colle et al. 1999). Since initial hydrologic states are carried forward for subsequent forecasts, this error accumulated and affected subsequent hydrologic forecasts. An experiment that evaluated the effect of using observation-based hydrological initial states, rather than those from previous mesoscale model forecasts, revealed that peak flow errors were reduced by approximately 50% by the use of these more accurate hydrologic initial states. This is a very important point, as this procedure can be performed in real time and can significantly reduce the error in the runoff forecast. Certainly, subsequent assessments of the UW system will include a more thorough validation of this as well as other real-time updating procedures.

The method of removing the long-term precipitation bias from the MM5 precipitation fields did not prove worthwhile for peak flow forecasting, at least in its current form. It appears that the MM5 precipitation bias is time (regime) dependent; furthermore, as noted in Colle et al. (1999, 2000), during the heaviest events the overprediction bias may be much smaller than during other periods. The no-bias forecast had the lowest average mass balance error, defined as the ratio of the model-predicted to observed discharge integrated over the 6-month period. The use of this correction scheme may therefore be useful in the prediction of other hydrological phenomena, such as maximum snowpack, summer low flow, and monthly or seasonal runoff. This could be especially useful for longer-term climate-related studies, where the accurate forecasting of significant

² The observation-based forecast obviously has less uncertainty than the other forecasts evaluated, since the others are based on predicted rather than observed meteorological conditions.

flow events may be secondary to determining the long-term (monthly or longer) discharge from a watershed.

The results from the control forecast are especially encouraging, particularly when one considers that the system as described in this study was not updated with observations, hence allowing MM5 forecast errors to accumulate and adversely affect later forecasts. It is noted that the statistics for the control forecast were significantly degraded by the poor meteorological forecast over the Sauk River during the three November events. In fact, if the Sauk River system is excluded from the overall statistics, the control forecasts become the most accurate of the four tested, with an average error of 25%.

The study also revealed other relevant results regarding peak flow forecasting. For example, the successful translation of calibration parameters to other gauges within the calibration basin and to adjacent basins (without recalibration) underscores a capability for forecasting in regions where gauge data are absent. This capability could be extremely beneficial not only in data-sparse regions throughout the western United States, but also in various regions throughout the world. The strong dependence of forecast runoff to input precipitation also highlights the necessity of accurate quantitative precipitation forecasts and the associated need to identify and rectify the deficiencies of atmospheric modeling systems, such as problems in microphysical schemes. Simple correction schemes based on long-term biases of the atmospheric model reduced the forecast skill of the system for individual events. Alternatively, more sophisticated corrections schemes (e.g., schemes that could further subdivide precipitation biases and spatial patterns based on mid-tropospheric wind speed and direction) may provide better bias correction. Assimilation of observations in real time continues to be problematic, but inclusion of these observations can lead to considerable (e.g., 50% reduction in forecast error on the Sauk River) improvement of forecast skill during major runoff events.

The synoptic skill of any particular atmospheric forecast can be a major source of error in the streamflow forecast. Methods that account for this atmospheric uncertainty, such as ensemble-based atmospheric forecasts, may significantly reduce the errors due to a single poor synoptic forecast, as occurred over the Sauk River watershed in November. The integration of mesoscale ensembles, and the subsequent reduced dependence on any single set of forecast conditions, would help to minimize the effect of a single poor forecast. Long-term testing of this type of system is currently being conducted at the University of Washington.

Acknowledgments. This research was supported by the National Oceanic and Atmospheric Administration (NOAA Cooperative Agreement NA67RJ0155) as well as the University of Washington Puget Sound Regional Synthesis Model (PRISM) project, which is supported

by the University Initiative Fund (UIF). Use of the MM5 was made possible by the Microscale and Mesoscale Meteorological Division of the National Center for Atmospheric Research, which is supported by the National Science Foundation. Special thanks to Mr. Doug McDonnal of the National Weather Service Forecast Office—Seattle, Dr. Bart Nijssen of the University of Washington Civil and Environmental Engineering Department, and Mr. Harvey Greenberg of the University of Washington Geological Sciences Department.

APPENDIX

Method of Determining the Long-Term Precipitation Bias in MM5 Spatial Precipitation Fields

The 13–24-h forecasts from all the real-time MM5 forecasts between October 1997 and May 1998 were aggregated. An analysis region was defined encompassing the MM5 4-km-resolution domain. The long-term precipitation bias was determined for 104 precipitation gauges within the analysis region. The area-weighted model precipitation bias B for the analysis region was given by

$$B = \frac{1}{AP} \sum_{i=1}^N p_i b_i a_i,$$

where b is the bias at the precipitation gauge, a is the area of a Thiessen polygon, p is the total volume of annual precipitation within the polygon, P is the total volume of water that falls over all the Thiessen regions, and A is the total area of all the Thiessen regions. The assumption in this approach is that each individual site bias is valid for a region surrounding the observation, which is a reasonable approach given sufficient gauge density. Since undercatchment of precipitation due to various environmental and instrumental factors was not accounted for, a regionwide adjustment where a 15% undercatchment was assumed was applied. Using this approach, it was determined that the MM5 model had an area-weighted bias of 1.52 throughout the integration region.

Determining the long-term precipitation bias in the MM5 precipitation fields requires accurate precipitation climatology of the region. The PRISM-derived precipitation climatology (Daly et al. 1994) is felt to be the best available for the region. A mass balance analysis of the PRISM-produced climatology fields with historical hydrographs revealed that there could be substantial underestimate of precipitation in many of the headwater regions in the western Cascades. It was also found that the MM5 tended to capture the distribution of precipitation in many of these headwater regions. Therefore, in an effort to retain some of this information from the MM5, the estimated “true” precipitation climatology used a weighted average of the PRISM-derived precipitation and the climatology produced by the MM5 for

the winter seasons from October 1997 through March 1999. Here, P_{true} is given by

$$P_{\text{true}} = aP_{\text{PRISM}} + bP_{\text{MM5}},$$

where P_{prism} is the 1961–90 PRISM-derived climatology and P_{MM5} is the normalized, bias-corrected MM5 climatology, and the coefficients a and b are given by 2/3 and 1/3, respectively. The long-term MM5 correction field is then given by

$$C = \frac{P_{\text{MM5}}}{P_{\text{true}}}$$

for any given grid point. The approach assumes that the areal region of integration is large enough that significant biases in the relative mass of water are insignificant. It should also be noted that this approach produced a bias field that agreed closely with the point values noted in Colle et al. (1999).

REFERENCES

- Bowling, L. C., P. Storck, and D. P. Lettenmaier, 2000: Hydrologic effects of logging in western Washington, United States. *Water Resour. Res.*, **36**, 3223–3240.
- Colle, B. A., K. J. Westrick, and C. F. Mass, 1999: Evaluation of the MM5 and Eta-10 precipitation forecasts over the Pacific Northwest during the cool season. *Wea. Forecasting*, **14**, 137–154.
- , C. F. Mass, and K. J. Westrick, 2000: MM5 precipitation verification over the Pacific Northwest during the 1997–99 cool seasons. *Wea. Forecasting*, **15**, 730–744.
- Daly, C., R. P. Neilson, and D. L. Phillips, 1994: A statistical-topographic model for mapping climatological precipitation over mountainous terrain. *J. Appl. Meteor.*, **33**, 140–158.
- Dudhia, J., 1989: Numerical study of convection observed during the Winter Monsoon Experiment using a mesoscale two-dimensional model. *J. Atmos. Sci.*, **46**, 3077–3107.
- Grell, G. A., J. Dudhia, and D. R. Stauffer, 1995: A description of the fifth-generation Penn State/NCAR Mesoscale Model (MM5). NCAR Tech. Note NCAR/TN-398+STR, 122 pp.
- Groisman, P. Y., and D. R. Legates, 1994: The accuracy of United States precipitation data. *Bull. Amer. Meteor. Soc.*, **75**, 215–227.
- Hong, S. Y., and H. L. Pan, 1996: Nonlocal boundary layer vertical diffusion in a medium-range forecast model. *Mon. Wea. Rev.*, **124**, 2332–2339.
- Kain, J. S., and J. M. Fritsch, 1990: A one-dimensional entraining/detraining plume model and its application in convective parameterization. *J. Atmos. Sci.*, **47**, 2784–2802.
- Miller, D. A., and R. A. White, 1998: A conterminous United States multilayer soil characteristics dataset for regional climate and hydrology modeling. *Earth Interactions*, **2**. [Available online at <http://EarthInteractions.org>.]
- Miller, N. L., and J. Kim, 1996: Numerical prediction of precipitation and river flow over the Russian River watershed during the January 1995 storms. *Bull. Amer. Meteor. Soc.*, **77**, 101–105.
- Mote, P. M., and Coauthors, 1999: Impacts of climate variability and change on the Pacific Northwest. JISAO/SMA, 108 pp. [Available from JISAO/SMA Climate Impacts Group, University of Washington, Box 354235, Seattle, WA 98195-4235.]
- Redmond, K., 2000: Verification of the Mt. Baker world record snowfall in 1999. *Proc. 68th Annual Meeting of the Western Snow Conference*, Port Angeles, WA, 58–63.
- Scott, J. M., and M. D. Jennings, 1998: Large-area mapping of biodiversity. *Ann. Mo. Bot. Gard.*, **85**, 34–47.
- Steenburgh, J. W., C. F. Mass, and S. A. Ferguson, 1997: The influence of terrain-induced circulations on wintertime temperature and snow level in the Washington Cascades. *Wea. Forecasting*, **12**, 208–227.
- Storck, P., and D. P. Lettenmaier, 1999: Predicting the effect of a forest canopy on ground snow pack accumulation and ablation in maritime climates. *Proc. 67th Annual Western Snow Conf.*, South Lake Tahoe, CA, 1–12.
- , —, B. A. Connelly, and T. W. Cundy, 1995: Implications of forest practices on downstream flooding, Phase II final report. Washington Forest Protection Association TFW-SH20-96-001, 100 pp. [Available from WPPA, 724 Columbia St. NW, Suite 250, Olympia, WA 98501.]
- , L. Bowling, P. Wetherbee, and D. Lettenmaier, 1998: Application of a GIS-based distributed hydrology model for the prediction of forest harvest effects on peak streamflow in the Pacific Northwest. *Hydrol. Processes*, **12**, 889–904.
- Sumioka, S. S., D. L. Kresch, and K. D. Kasnick, 1998: Magnitude and frequency of floods in Washington. Resources Investigations Rep. 97-4277, United States Geological Survey Water, 91 pp. [Available from USGS Information Services, Box 25286, Denver Federal Center, Denver, CO 80225-0046.]
- Tangborn, W. V., and L. A. Rasmussen, 1976: Hydrology of the north Cascades region, Washington 1, Runoff, precipitation, and storage characteristics. *Water Resour. Res.*, **12**, 187–202.
- Westrick, K. J., and C. F. Mass, 2001: An evaluation of a high-resolution hydrometeorological modeling system for prediction of a cool-season flood event in a coastal mountainous watershed. *J. Hydrometeorol.*, **2**, 161–180.
- , —, and B. A. Colle, 1999: The limitations of the WSR-88D radar network for quantitative precipitation estimation over the coastal western United States. *Bull. Amer. Meteor. Soc.*, **80**, 2289–2298.
- Wigmosta, M. S., L. W. Vail, and D. P. Lettenmaier, 1994: A distributed hydrology–soil–vegetation model for complex terrain. *Water Resour. Res.*, **30**, 1665–1679.
- Yang, D., B. E. Goodison, J. R. Metcalfe, V. S. Golubev, R. Bates, T. Pangburn, and C. L. Hanson, 1998: Accuracy of NWS 8" standard nonrecording precipitation gauge: Results and application of WMO intercomparison. *J. Atmos. Oceanic Technol.*, **15**, 54–68.